THE INTERPLAY BETWEEN MAGNETISM AND SUPERCONDUCTIVITY IN RNi_2B_2C (R=Lu, Tm, Er,Ho, Dy, Tb, Gd)

M. El Massalami, S.L. Bud'ko, B. Giordanengo, and E.M. Baggio-Saitovitch.

CBPF, R.Xavier Sigaud 150, 22290-180, Rio de Janeiro, Brazil

ABSTRACT

The superconducting and magnetic phase diagram (characteristic temperatures *versus* effective ionic-radii) of the RNi_2B_2C (R=Lu,Tm,Er,Ho,Dy,Tb,Gd) compounds are considered. Although the gradual degradation of superconductivity can be scaled to the de Gennes factor, $(g-1)^2J(J+1)$, the unique reentrant behavior of the $HoNi_2B_2C$ compound and the abrupt quenching of superconductivity for R lighter than Ho are most probably unaccountable within this scheme. Rather, it is argued that their low-T magnetic and transport properties as well as the main features of the interplay between magnetism and superconductivity can be accounted for if the low-T magnetism of $HoNi_2B_2C$, as reported by T.E. Grigereit et al, is generalized to the other isomorphous R-members. Thus the onset of the 4f-moments antiferromagnetic state at T_1 is accompanied by an oscillatory component, which transforms to a commensurate antiferromagnetic state at T_2. For HoNi2B2C, the pressure and magnetic field influence on T_c, T_1 and T_2 will be discussed.

1. Introduction

The structure of the new boro-carbide RNi_2B_2C (R=Y, rare earth) compounds [1-3] can be viewed as a stacking of (super-) conducting Ni_2B_2 layers that are spatially separated by RC planes. The R-size variation was found to entail systematic changes in the intra- and inter-layer distances[2] with a consequent systematic R-dependence of the magnetic and the transport properties. When R carries a magnetic moment, such a structural arrangement is a realization [3-15] of yet another family of compounds [16-19] wherein the R-dependent strength of the superconductivity-magnetism interplay leads to a de Gennes-type T_c-degradation as well as causing the series to pass through different type of behaviors: coexistence, reentrant or normal-state regime. In particular, the $HoNi_2B_2C$ compound (for $T<T_c=7.5K$) showed a reentrant to the normal-state transition at $T_1\sim 6K$, followed at $T_2 \sim 4K$ by a comeback to the superconducting state[4,5].

This unique behavior (referred to below as a reentrant-comeback) leads to a characteristic dip structure in the $H_{c2}(T)$ curve [4]. Of course, the de Gennes scaling arguments would not be sufficient to account for such a unique behavior. Rather, the neutron diffraction studies[5] showed that it is related to the helical state which, at lower temperatures, transforms to a commensurate antiferromagnetic state in which superconductivity is restored. This picture will be shown below to give an adequate account of the low-T magnetic and transport properties and the interplay between magnetism and superconductivity in the RNi_2B_2C compounds.

In Ref.8 and 14 we have used this picture to explain the magnetic and superconducting properties of the pseudo-quaternary series (Y,Gd)Ni_2B_2C wherein the influence of the pair-breaking paramagnetic centers (Abrikosov-Gorkov picture) is responsible for the linear lowering of T_c. We were able to outline the coexistence, the reentrant, and the normal-state regime and, moreover, show that the quenching of superconductivity is related to the adverse magnetic influence on the Cooper-pairs.

The format of this paper will be as follows. In Sec.2, we will review briefly the current experimental situation (see Ref.[3-15] for more details) while the discussion and conclusions are given, respectively, in Sec.3 and Sec.4.

2. Review of the experimental results

The normal-state resistivity, ρ, of these compounds showed a metallic behavior with dominant electron-phonon scattering down to 30K [3,4,8,10], below that, a T-independent resistivity was observed. At even lower temperatures, Cava et al [4] reported that a superconducting transition occurred for R= Y, Lu, Tm, Er and Ho. (see Fig.1). For $HoNi_2B_2C$, a reentrant behavior was observed at T_1=5.7K with a subsequent comeback to superconductivity at T_2 =3.8K even at zero applied field. The zero-field ρ-T ($T<T_c$) for R=Tm, Er do not show any reentrant-comeback behavior. Moreover, Fig.1 also shows that increasing H_{ap} is found to shift down T_c and broaden the temperature range, $\Delta T = T_1 - T_2$, of the reentrant-comeback region.

For R = Dy, Tb, Gd, a remarkable anomalous nonsuperconducting lowering of ρ(T) was observed (see Fig.2). The onset point of the latter coincided with the onset-point of a magnetic transition, thus conclusively asserting its magnetic origin [4,8]. Due to the onset of superconductivity in the R=Tm, Er, Ho compounds, well above the onset of the magnetic transitions, such an anomalous behavior in ρ-T could be recovered only for an applied field $H_{ap} > H_{c2}$ (see Fig.1 [4])

The high-T magnetism of these compounds showed that the Curie- Weiss 4f-paramagnetism (with the free-ion μ_{eff}) was strictly followed with positive θ (except for R=Tm) indicating a dominant ferromagnetic interactions [3,4,6,8]. From μ_{eff} values, it was concluded that the Ni-ions were not contributing (at least not appreciably) to the magnetism of these compounds. As the temperature was decreased, superconducting or magnetic transitions were observed.

As an additional confirmation of the zero-field reentrant-comeback behavior for the $HoNi_2B_2C$, Schmidt and Braun reported the χ_{ac}-T curve (Fig.3) where superconductivity was seen to set-in at T_c=7.2K, the normal state is reentered at T_1 and superconductivity is restored at T_2. In addition Fig.(3) shows also the influence of the physical pressure on T_c, T_1 and T_2. As evident, T_c was shifted downwards while both T_1 and T_2 were weakly shifted upwards.

Superconductivity was not detected down to 1.5K (see Fig.2) for R=Tb,Gd and to 300mK for R=Dy[10]. Rather, for these compounds, two magnetic transitions were observed: e.g. for R=Gd, at T_1= 19.0±0.5K (Fig.4) and at T_2=7.2±0.3K (Fig.4). Similar transitions were also observed for $HoNi_2B_2C$

(Fig.5), $TbNi_2B_2C$ and $DyNi_2B_2C$. From the neutron diffraction [5], magnetization measurements [13-15] and specific heat [6,9] the T_1 peak can be attributed to an antiferromagnetic (ANFMGT) transition which is accompanied (or preceded) by a helical arrangement. Evidently, the Zero Field Cooled (ZFC) and Field Cooled (FC) features appearing in the M-T curves (e.g. for R=Gd,Ho see Fig.4-5 respectively) can be associated with such a helical spin arrangement of the strong planar ferromagnetism. As mentioned above, the neutron diffraction studies on the $HoNi_2B_2C$ [5] revealed such a helical spin arrangement. Moreover, it was shown that such a non commensurate spin state transformed at T_2 into a commensurate antiferromagnetic state. We then attribute the T_2 peak (which was observed for R=Tb, Dy, Gd) to such a transition (which is probably of the first-order type).

The high-field magnetization measurements [13-15] demonstrated that the crystal field anisotropy for R=Ho, Gd are negligible and both systems could be considered as Heisenberg antiferromagnets. In addition, the insets in Fig.4 and in Fig.5 shows that the magnetic moment per R-ion saturates to the theoretically expected values. This conclusively demonstrates the negligible magnetic contribution of the Ni-ions in these compounds. Moreover, the saturation field is found to be 3.8T for R=Ho and 13.3(3)T for R=Gd. This indicates that the exchange coupling are quite strong and in fact explains the observed weak dependence of the magnetic transitions (T_1 and T_2) on the application of the magnetic field [Fig.1] and hydrostatic pressure [Fig.3]. However, the relatively strong influence of both parameters on the superconducting transition (T_c) is coupled to their influence on the helical state as will be discussed below.

The overall low-T features of RNi_2B_2C (relevant to our purpose) is summarized in the phase diagram shown in Fig.6., wherein the superconducting (T_c) and the magnetic transition temperatures (T_1,T_2) are plotted against the effective R^{+3}-ionic radius. An alternative rationalization in terms of the de Gennes factor or lattice metric properties can be undertaken [4], since the factor $(g-1)^2J(J+1)$, the lattice parameters and the R-size are varying monotonically across the rare earth ions under study (see Fig.6.b). We argue that the present scaling in terms of the R-ionic radius is justified by the structural studies[2]. There, it was found that R-size variation gives rise to a monotonic variation in the lattice parameters (see Table.1) which is expected to give rise to monotonic changes in the superconducting and magnetic properties. A clear evidence of the size variation is shown in Fig.6.b for the R=Lu, Y where size effect rather than magnetic perturbations are leading to T_c degradation.

Fig.7 shows a remarkable peak in the χ_{ac}-T for R=Dy, Tb, Gd at low temperatures indicating an onset of an additional magnetic transition. Moreover, we observed a similar features in some of the $HoNi_2B_2C$ and YNi_2B_2C samples. Such a behavior was also reported for $LuNi_2B_2C$ (T=2K[7.a,12]) and $ErNi_2B_2C$ (T=2.2K,[9]) and was thought to be associated with the ordering of the fluctuating Ni moments [7.a]. However, as can be seen in Fig.8, these transitions showed no systematic trend across the R-series and most probably were due to non-R containing impurity phase.

3. Discussion

Based on the above mentioned structural features and assuming the indirect exchange model, the intra-plane coupling (J_i) is expected to be stronger than the far-separated inter-planar coupling (J_o) and the strength of both should depend on the R-size and on the magnitude of the factor $(g-1)^2J(J+1)$ (J=total angular momentum and g is the g-factor). Consequently, on increasing the R-size, the T_1 ordering temperature was found to increase and to follow de Gennes scaling as shown by the solid line in Fig.6.a.

Similar arguments imply that increasing the R-size would bring the 4f-moments closer to the (super)-conduction electrons at the Ni layers. This is expected to enhance the hybridization of the 4f states with the valence states. Then the transport properties in the normal- and the superconducting-state will depend not only on the de Gennes factor but also on the R-size variation [20]. Such a size effect (which is clearly seen in Fig.6.b) is most probably influencing T_c by a decrease (although weakly) in $N(E_F)$ on shifting of the position of the Fermi level.[21-22]. On the other hand, the de Gennes factor is shown in Fig.6.a to scale for T_c and for the onset point of the anomalous drop in ρ-T curves.

To account for the reentrant-comeback behavior in $HoNi_2B_2C$, in particular, and the interplay features, in general, we extend the magnetic picture that was developed for $HoNi_2B_2C$ [5] to the RNi_2B_2C compounds:- the 4f-moments are strongly coupled ferromagnetically within the planes (J_i) and weakly out of plane (J_o). The latter coupling leads to a 3-dimensional antiferromagnetic order at T_1, however, with a noncollinear helical state which would transform to a commensurate antiferromagnetic state at T_2.

In this picture, the adverse influence on the superconducting pairs of the unbalanced exchange magnetic field at the Ni-layers (as a result of the helical state) is the origin of the reentrant features in $HoNi_2B_2C$ [5]. Due to the subsequent onset of the collinear antiferromagnetic state at T_2, superconductivity can be restored. From Fig.6.a, the T_1 line is clearly associated with this reentrant behavior at R=Ho. In fact this is an indirect evidence of the presence of the helical component: if T_1 is purely antiferromagnetic in character, then coexistence rather than reentrant behavior should be expected.

As seen in Fig.2, no zero-field reentrant-comeback behavior is observed for R = Tm, Er [4,5]. Rather, the specific heat measurements[6,9] and μ^+SR studies [7.a,12] showed them to be antiferromagnetic superconductors (see Fig.6.a) and , in zero field with only one magnetic transition point. Therefore, in zero field, the helimagnetic state is absent and so no reentrant behavior should be expected. However, the observed field-dependence of $\rho(T)$ is originating from the field dependence of T_N.

For R=Dy,Tb,Gd, the increase in the strength of the layered ferromagnetism is sufficient to quench superconductivity and to give rise to a measurable difference in the FC and ZF magnetization measurements (Fig.4-5).

In the $\rho(T)$ curves of RNi_2B_2C (R=Dy,Tb,Gd), an anomalous reduction of the electronic scattering is found to follow the T_1 ANFMGT order. As is well known, such a decrease is expected to occur when the effective magnetic correlation length is considerably longer than the effective electronic mean-free path ($\xi_m >> L$). Then, it is tempting to attribute such a decrease in ρ to the layered ferromagnetism which is well developed at the T_1 line.

The positive θ observed in the Curie-Weiss behavior of these systems can be related to the fact that for $T>T_1$, the dominant magnetic interactions are the stronger in-plane ferromagnetic couplings. In addition, these couplings are expected to lead to a pronounced short range order effects and, as shown in the experimental results [4,5,8], a deviation from CW-law starts well above T_1.

The helical state in $HoNi_2B_2C$ was shown in Ref.13 to be due to the competition between the out-of-plane interactions among the first and the second nearest planes, denoted respectively by J_{o1} and J_{o2}. By assuming planar spins and using Molecular Field Theory [23-24], the magnetic ground state of such a spin system is equivalent to that of a magnetic chain having nearest (J_{o1}) and next-nearest (J_{o2}) interactions and with a chain axis which is perpendicular to the ferromagnetic layers. Then, the helical configuration would be the lowest ground state if both J_{o1} and J_{o2} are of antiferromagnetic type and their ratio is less than 4. This is the case since

$$J_{o1}/J_{o2} = -4\cos(\theta) = -4\cos(16.4°+180°) \approx 3.84,$$

where the substituted value of the spiral angle, θ, is taken from Ref.5. Moreover, for an electron gas polarized by a plane of ferromagnetic aligned moments, the polarization strength decays with an $1/(r^2)$ dependence (where r is the interplanar separation). This dependence yields $J_{o1}/J_{o2} \approx 4$ in good agreement with the value determined experimentally from the above equation.

It is most likely that, the application of a magnetic field (for $H_{app} < H_c < H_{sat}$) or a physical pressure would affect the delicate balance among these competing exchange interactions (J_{o1} and J_{o2}). This would hardly influence the magnetic transitions (T_1 and T_2, since $H < H_{sat}$), however, would drastically modify the accompanying helical spin arrangement. Consequently, influences the superconducting pairs through the unbalanced exchange field at the Ni-sheets. This is evident in the $\rho(H)$-T curves of Fig.2 and the $\chi(P)$-T of Fig.3.

The fact that the helical state and the superconducting state are excluding each other can be observed clearly in Fig.6.a. In fact the depairing of the Cooper pairs by the helical state produces additional electrons to intermediate and hence strengthen the magnetic coupling between the planes. This is exhibited clearly for the R = Ho[$T_2 < T < T_1$], Dy, Tb, Gd compounds. Conversely, the pairing of the conduction electrons leads to a decrease in the number of conduction electrons ready to participating in the magnetic coupling and so minimize the possibility of the helical state. This is the case for R=Tm,Er,Ho[$T < T_2$]

4.0 CONCLUSION

In the RNi_2B_2C compounds, the structural features as well as the R-ion magnetism have a decisive influence on the resulting superconducting and magnetic properties and the interplay between these two phenomena. It is stressed that although the de Gennes scaling could be used to interpret the T_c-drop in RNi_2B_2C, such a mechanism is not able to explain the unique reentrant-comeback behavior which was observed in $HoNi_2B_2C$ and the abrupt absence of superconductivity for R lighter than Ho. We have shown that the magnetic features of these systems can be interpreted by assuming a strong in-plane ferromagnetic coupling and a weak interplanar antiferromagnetic couplings among the 4f-moments resulting in a magnetic order, however, with a spiral spin arrangement. The latter would transform to a commensurate antiferromangetic order at a lower temperatures. Such a magnetic description, which had been already probed by neutron diffraction studies on the $HoNi_2B_2C$ system, was shown in this work to account qualitatively for the observed phase diagram features in the RNi_2B_2C compounds.

Finally, More studies, such as low-T single crystal magnetic studies, neutron powder diffraction, rare earth Mossbauer measurement, would be needed to confirm the spin structure and its influence on the superconductivity in these systems.

ACKNOWLEDGMENT

We gratefully acknowledge the critical reading and the fruitful discussions we have with Profs. W. Baltsberger, M. A. Continentino, D. Ellis, A. Gomes, P.Kess and H. R. Ott. M. B. Fontes and J. Mondragon are acknowledged for experimental assistance. This work was supported by RHAE program on New Materials (MCT), CNPq grant #5.00938/91-1. M.E was supported by a FAPERJ fellowship.

Table Captions

Tab.1

Representative lattice lengths for the RNi_2B_2C (R=Lu,Y and Gd) compounds. The Ni-Ni distances are comparable to the Ni-metal Ni-Ni distances (2.5Å), stressing the metallic character of the Ni-sheets. Data are taken from Ref.[2,8].

parameter(Å)	Lu	Y	Gd	
a	3.464	3.526	3.577	
c	10.631	10.533	10.36	
$R\text{-}R = a$	3.464	3.526	3.577	in-plane
$R\text{-}R = \frac{1}{2}\sqrt{(2a^2 + c^2)}$	5.853	5.827	5.764	off-plane
$Ni\text{-}Ni = a / \sqrt{2}$	2.449	2.493	2.529	in-plane
$Ni\text{-}Ni = c/2$	5.316	5.217	5.13	off-plane

References

[1] R. Nagarajan, C. Mazumdar, Z. Hossein, S.K. Dhar, K.V. Golpakrishna, L.C. Gupta, C. Godart, B.D. Padalia and R. Vijayaragharan, Phys.Rev.Lett. 72(1994)274.

[2] T. Siegrist, H.W. Zandbergen, R.J. Cava, J.J. Krajewski and W. F.Peck, Nature 367 (1994) 252; H.W. Zandbergen, R.J. Cava, J.J. Krajewski, W.F. Peck, Jr., Physica C224(1. 1994)6.

[3] R.J. Cava, H. Takagi, B. Batlogg, H.W. Zandbergm, J.J. Krajewski, W. F. Peck, Jr, T. Siegrist, B. Batlog, R. B. van Dover, R. J. Felder, K. Mizuhashi, J.O. Lee, H. Eisaki, and S. Uchida, Nature 367(1994)252.

[4] H. Eisaki, T. Takagi, R.C. Cava, K. Mizuhashi, J.O. Lee, B. Batlogg, J.J. Krajewski, W.F. Peck and S. Uchida, Phys.Rev.B 50(1994)647.

[5] T.E. Grigereit, J.W. Lynn, Q. Huang, A. Santoro, R.J. Cava, J.J. Krajewski and W.F. Peck, Jr, preprint.

[6] R. Movshovich, M.F. Hundley, J.D. Thompson, P.C. Canfield, B.K. Cho, A.V. Chubukov, Physica C 227(1994)381.

[7] Reference in abstract form reported in *HT_C-update*: D.W. Cooke et al *HT_C-update* 8,#9(1994); S.A. Carter et al; *HT_C-update* 8,#9(1994) ,W.M. Hong; *HT_C-update* 8,#9(1994); M.Xu et al, 6,#9(1994), B.C. Chakoumakos and M. Parnthaman, *HT_C-update* 6,#9(1994)

[8] M.El Massalami, S.L. Bud'ko, B. Giordanengo, M.B. Fontes, J.C. Mondragon and E.M. Baggio-Saitovitch. to appear in M^2S proceedings, Grenoble (1994).

[9] H. Michor, W. Perthod, T. Holubar, N.M. Hong and G. Hilscher, to appear in M^2S proceedings, Grenoble (1994).

[10] C.V.Tomy, L.J. Chang, G. Balakrishnan and D.McK. Paul ;to appear in M^2S proceedings, Grenoble (1994)

[11] H. Schmidt and H.F. Braun preprint

[12]L.P. Le, R.H. Heffner, G.J. Niewenhuys, P.C. Canfiled, B.K. Cho, A. Amato, R. Feyerherm, F.N. Gygax, D. EMaclaughlin and A. Schenck preprint.

[13] M.El Massalami, B. Giordanengo, E.M. Baggio-Saitovitch and A. Sulpice submitted to Physica C.

[14] M.El Massalami, S.L. Bud'ko, B. Giordanengo, M.B. Fontes and E.M. Baggio-Saitovitch, to be submitted

[15] B. Giordanengo, M. El Massalami, S.L. Bud'ko, E.M. Baggio-Saitovitch, J.Voirn and A. Sulpice to be submitted

[16] A. Gootas et al Phys.Rev. B36(1987)7277; C.U. Segre and H.F. Braun, Phys.Lett. 85A(1981)372.

[17] D.C Johnston and H.F. Braun; in : Superconductivity in ternary compounds II, M.B. Maple and O. Fischer eds., Springer-Verlag, Berline,1982.

[18] S.V. Vonsovsky, Yu.A. Izyumov and E.Z. Kurmaev; Superconducitivity of transition metals (Springer series in Solid-state Sciences 27,N.Y., 1982; A.V. Narlikar and S.N. Ekbote, Superconductivity and superconducting materials, (South Asian Publisher-New Delhi,1983)

[19] G.K. Shenoy, B.D. Dunlap, F.Y. Fardin, S.K. Sinha, C. Kimball, W. Poptzel, F. Probst and G.M. Kalvius, Phys.Rev. B21(1980)3886.

[20] C. Kittel, Quantum Theory of Solids, (John Wiley and son, N.Y.,1987) p.364.

[21] W.E. Pickett and D.J. Singh, preprint

[22] L.F. Mattheiss, Phys.Rev. B49(1994).

[23] J.S. Smart, EffectiveField Theories of Magnetism ,(W.B.Saunders Company,1966) p.101.

[24] R.L. Carlin and A.J. van Duyneveldt, in Magnetic propeties of transition metal compounds, (springer-Verlag,N.Y.,1978) p.184;

Figure captions :-

Fig.1. The low-T resistivity under varying applied magnetic field for RNi_2B_2C (R=Ho, Er, Tm). The short vertical arrows emphasize the fact that, (for $H<H_{sat}=3.8T$), the peak position (taken as an indication of the magnetic transitions) is weakly sensitive to the applied field. Data taken from Ref.[4].

Fig.2. The low-temperature resistivity for R = Dy, Gd, Tb. (a) for $T > T_1$, the temperature independent resistivity was fitted to a polynomial function. This was subtracted from the polynomial-fit to the resistivity at $T<T_1$. (b) shows the magnitude of the anomalous lowering of the resistivity due to the magnetic order onset at T_1. For the sake of clarity, the R=Tb curve is stretched upwards.

Fig.3. The χ_{ac} -T of the $HoNi_2B_2C$ for different applied hydrostatic pressure . Notice the weak dependence of the magnetic transition points(T_1 ,T_2) on the applied pressure [data taken from Ref.11].

Fig.4. The Zero-Field Cooled (ZFC) and Field Cooled (FC) M/H-T in a field of 10 Oe for $GdNi_2B_2C$. The vertical arrows marks T_1 and T_2 transition points. The inset shows the magnetic moment per Gd- ion *versus* the applied field at T=1.7K.

Fig.5. The Zero-Field Cooled (ZFC) and Field Cooled (FC) M/H-T in a field of 10 Oe for $HoNi_2B_2C$. The inset shows the magnetic moment per Ho- ion *versus* the applied field at T=1.7.

Fig.6. (a) The magnetic (T_1, T_2) and the superconducting (T_c) transition temperatures of the RNi_2B_2C as a function of the effective R-ionic radius. The solid lines represents the de Gennes scaling for both the magnetic and superconducting experimental points.

(b) Comparison of the reduction in T_c expected from size effects (Lu,Y) with the relatively large reduction due to the 4f-magnetism (Tm,Er,Ho). The line joining Tm, Er and Ho is a de Gennes scaling of T_c., the other line is a guide to the eye. For completeness sake, the de Gennes factor for the magnetic R-ions is also displayed.

Data are taken from Ref.[3-6,8,9,,12,15-17].

Fig.7. The low-T χ_{ac} (T) curves of RNi_2B_2C (R=Dy,Tb,Gd). The sinusoidal field oscillates at 500Hz with an amplitude of 1 Oe. These peaks can be easily probed by the zero-field χ_{ac} measurement, however, they will be drastically influenced by a relatively small magnetic field.

Fig.8. The low temperature anomalous magnetic transition for RNi_2B_2C plotted as a function of the R-ionic radius. The horizontal dashed line (which is a fit to the experimental data) indicates the absence of systematic dependence on the R-ion type.

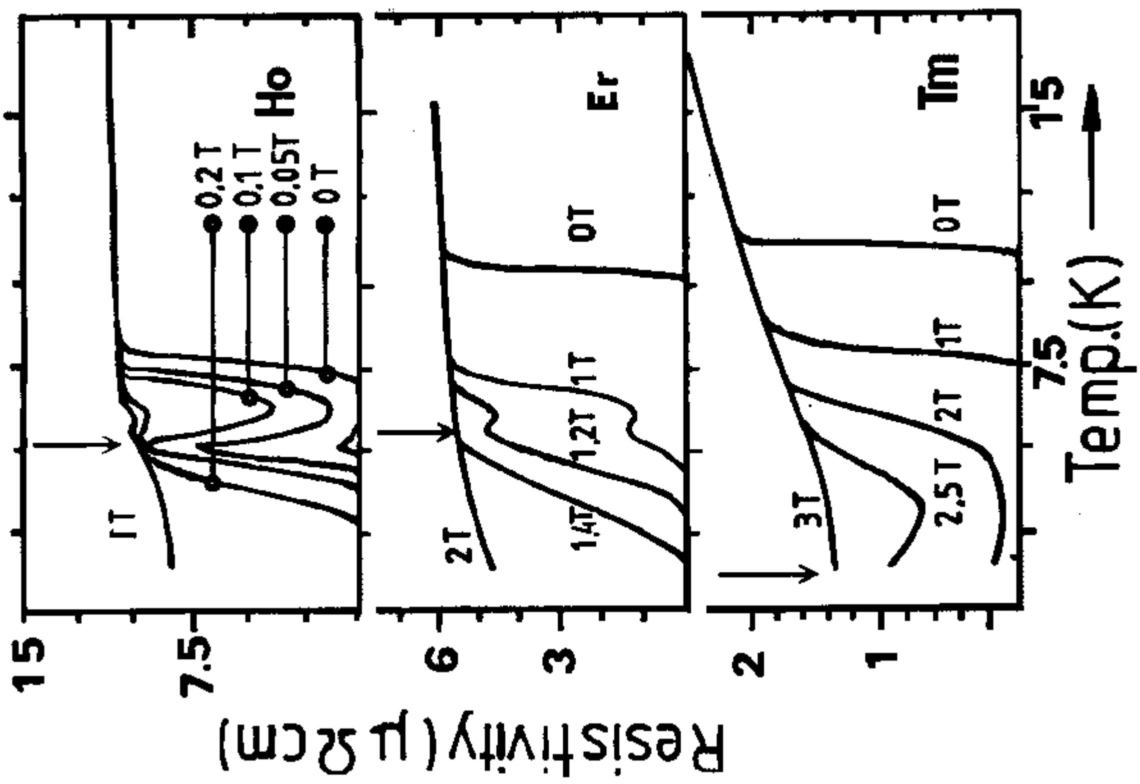
Resistivity (μ Ω cm)
15
7.5
6
3
2
1
Ho
0,2 T
0,1 T
0,05T
0T
1T
Er
2T
1,4T
1,2T
1T
0T
Tm
3T
2,5T
2T
1T
0T
7.5
15
Temp.(K)

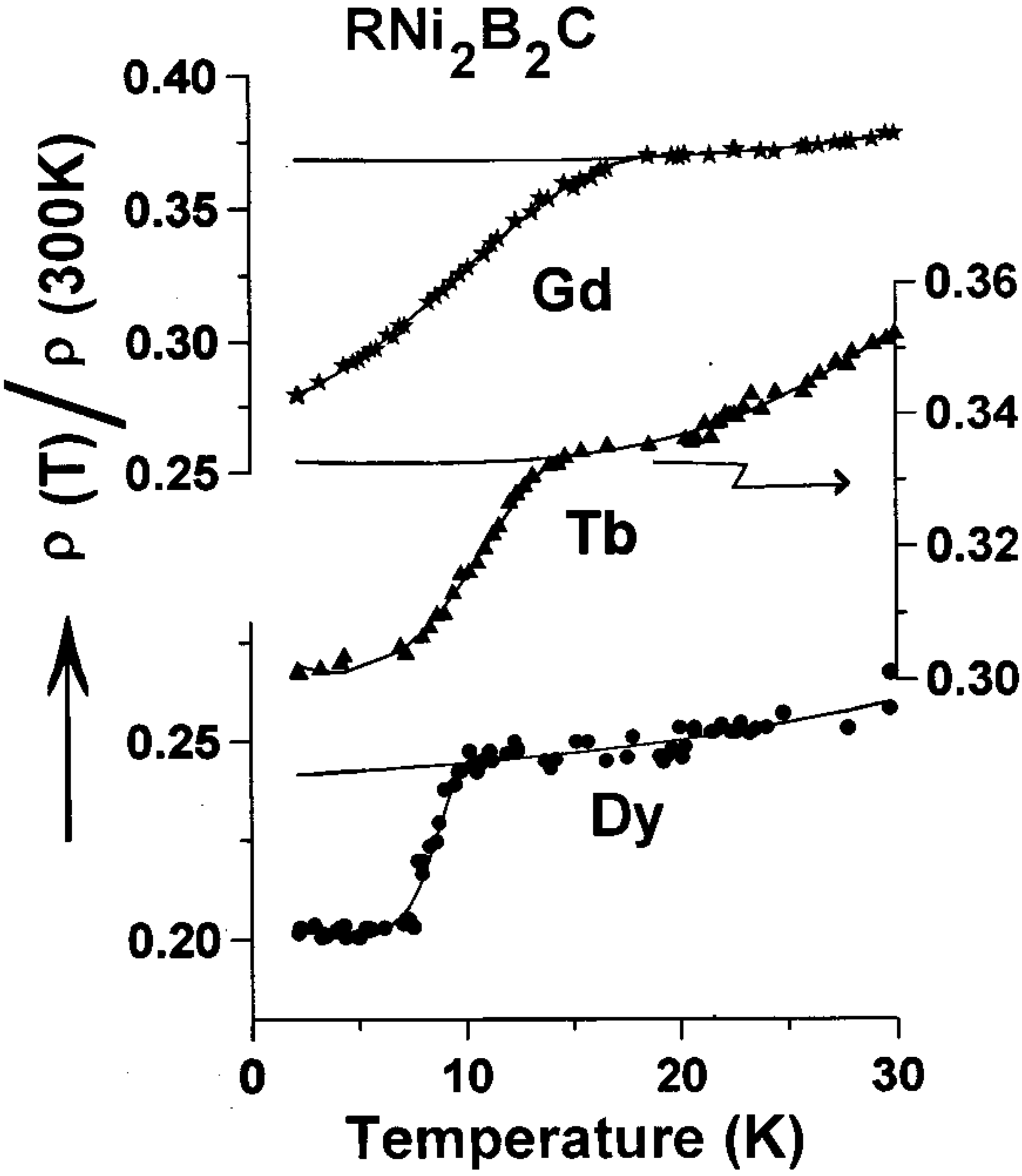
RNi_2B_2C
0.40
0.35
0.30
0.25
0.25
0.20
ρ (T) / ρ (300K)
Gd
Tb
Dy
0.36
0.34
0.32
0.30
0
10
20
30
Temperature (K)

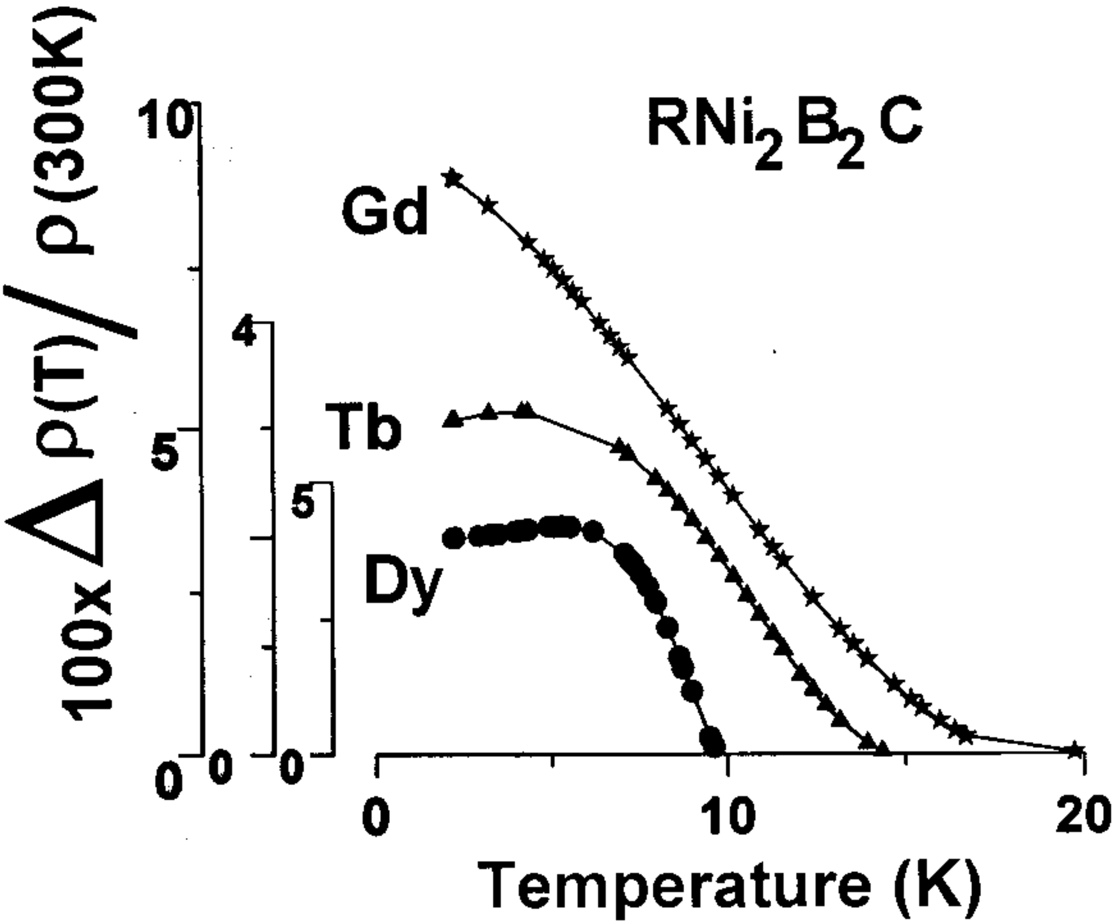
RNi$_2$B$_2$C
Gd
Tb
Dy
100x Δ ρ(T) / ρ(300K)
10
5
0
4
0
5
0
0
10
20
Temperature (K)

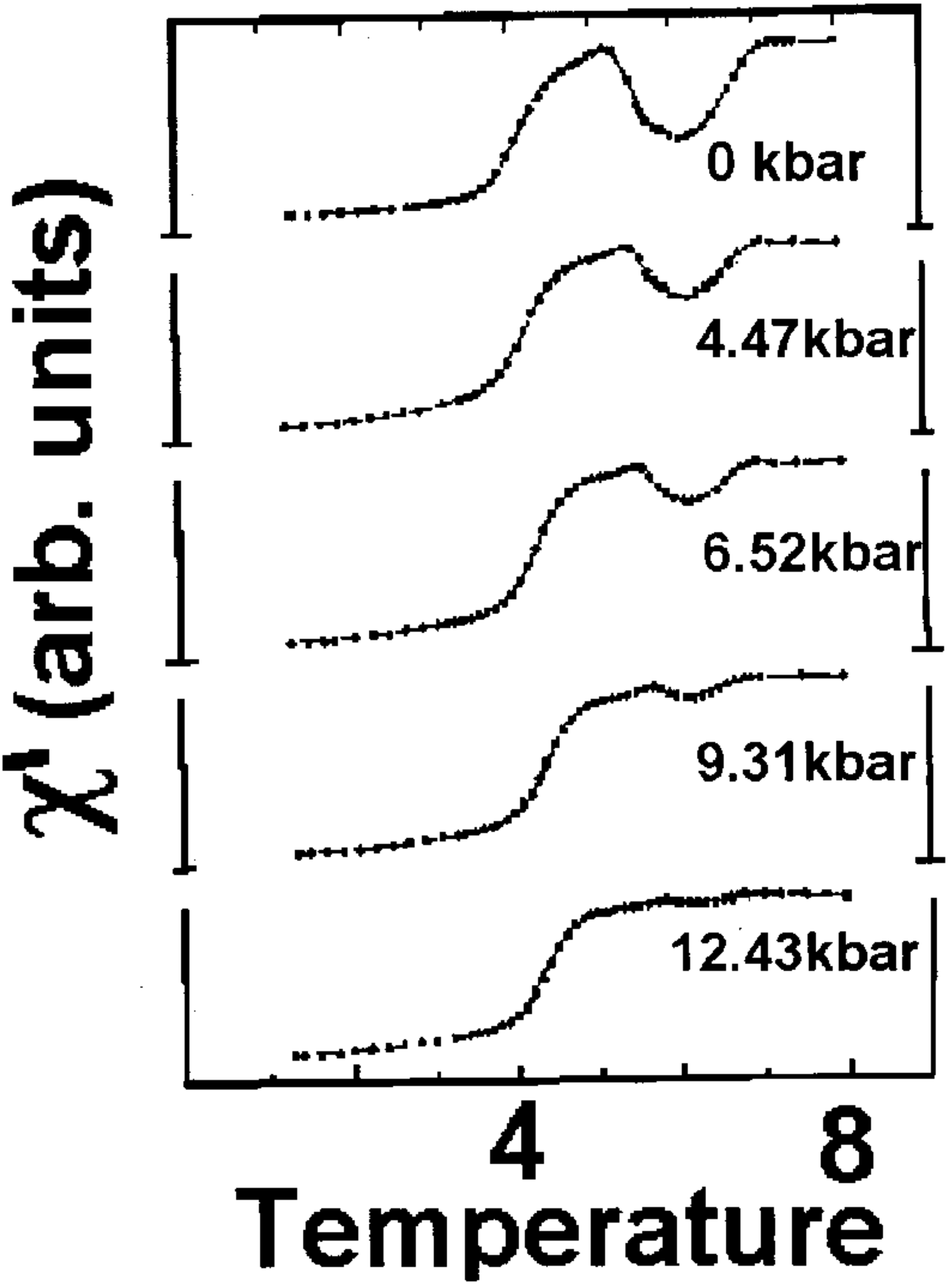
χ' (arb. units)
0 kbar
4.47kbar
6.52kbar
9.31kbar
12.43kbar
4
8
Temperature

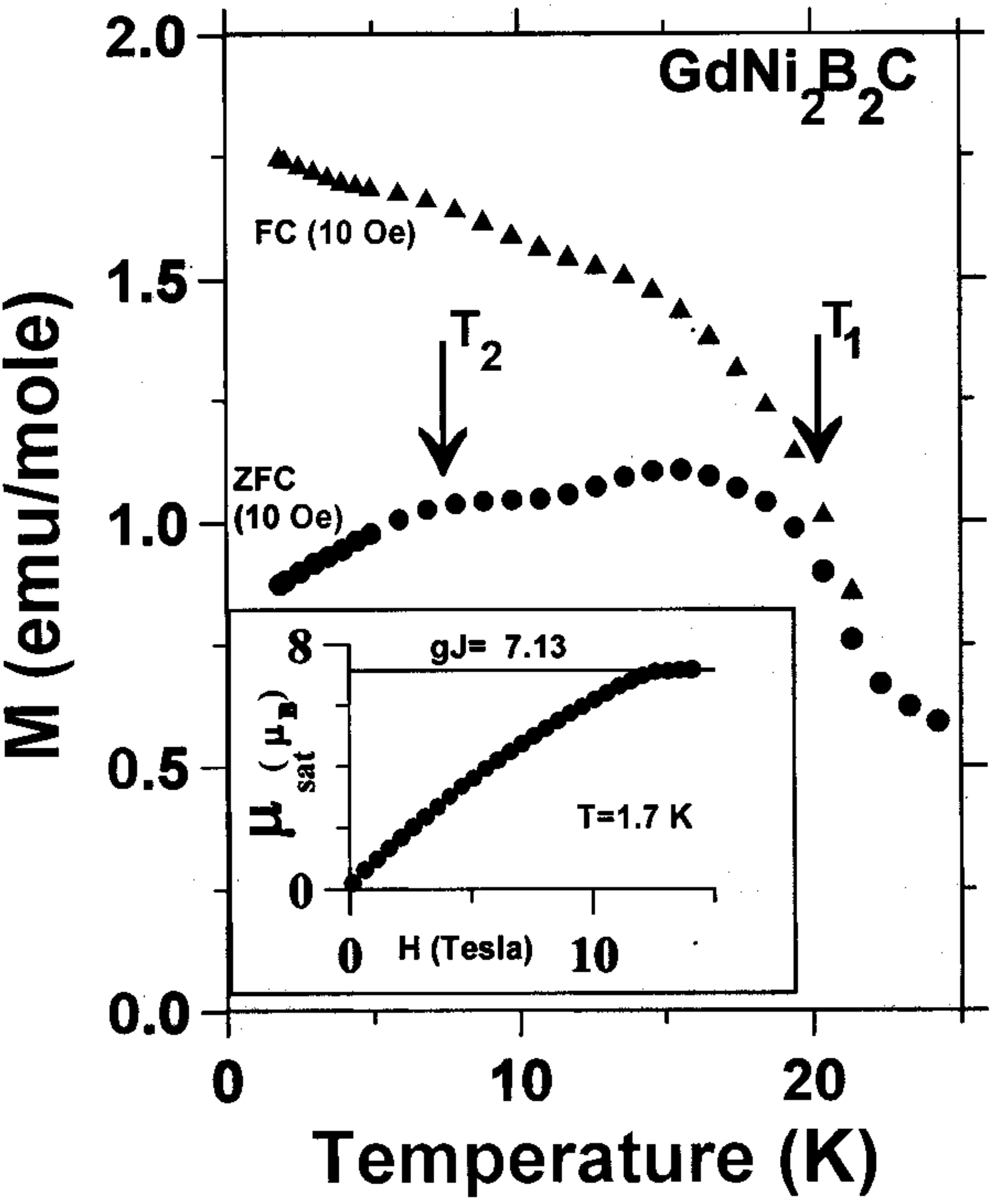
GdNi$_2$B$_2$C
M (emu/mole)
2.0
1.5
1.0
0.5
0.0
0
10
20
Temperature (K)
FC (10 Oe)
ZFC
(10 Oe)
T$_2$
T$_1$
8
0
μ_{sat} (μ_B)
gJ= 7.13
T=1.7 K
0
H (Tesla)
10

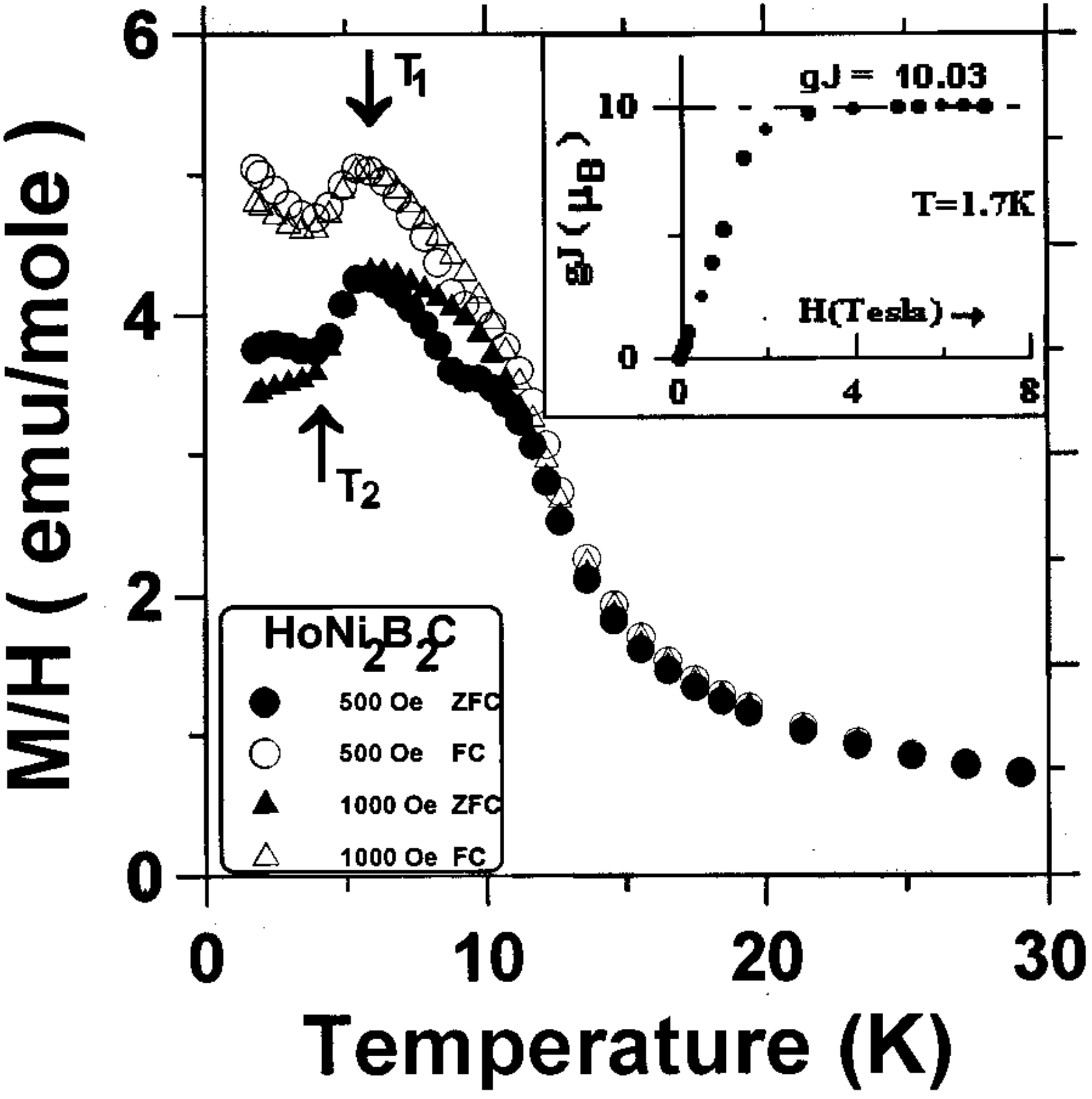
M/H (emu/mole)
Temperature (K)
0
2
4
6
0
10
20
30
T1
T2
HoNi2B2C
500 Oe ZFC
500 Oe FC
1000 Oe ZFC
1000 Oe FC
gJ = 10.03
gJ (μB)
10
0
T=1.7K
H(Tesla) →
0
4
8

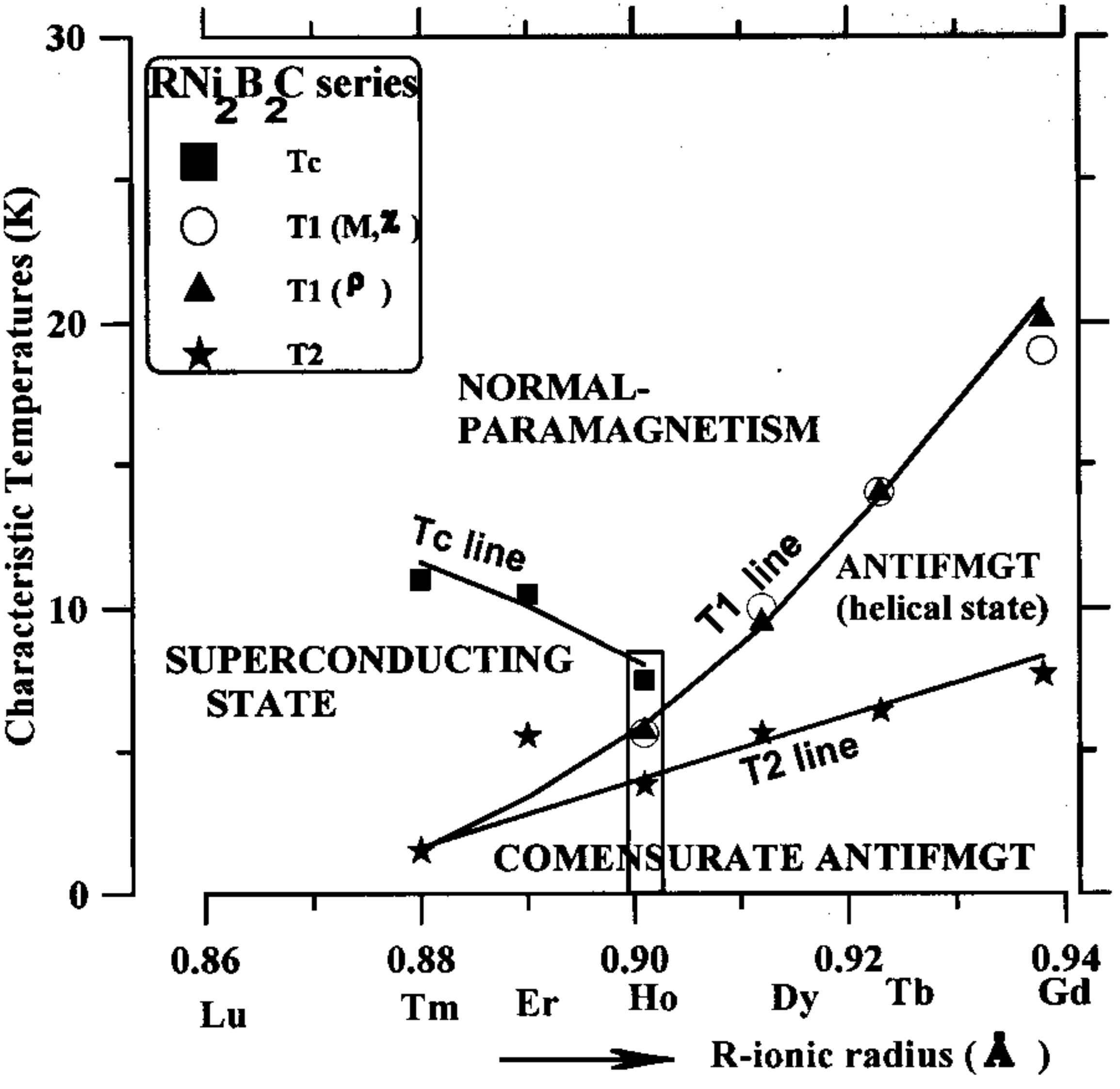
RNi2B2C series
■ Tc
○ T1 (M,χ)
▲ T1 (ρ)
★ T2
NORMAL-PARAMAGNETISM
Tc line
T1 line
T2 line
ANTIFMGT (helical state)
SUPERCONDUCTING STATE
COMENSURATE ANTIFMGT
Characteristic Temperatures (K)
0
10
20
30
0.86
0.88
0.90
0.92
0.94
Lu
Tm
Er
Ho
Dy
Tb
Gd
R-ionic radius (Å)

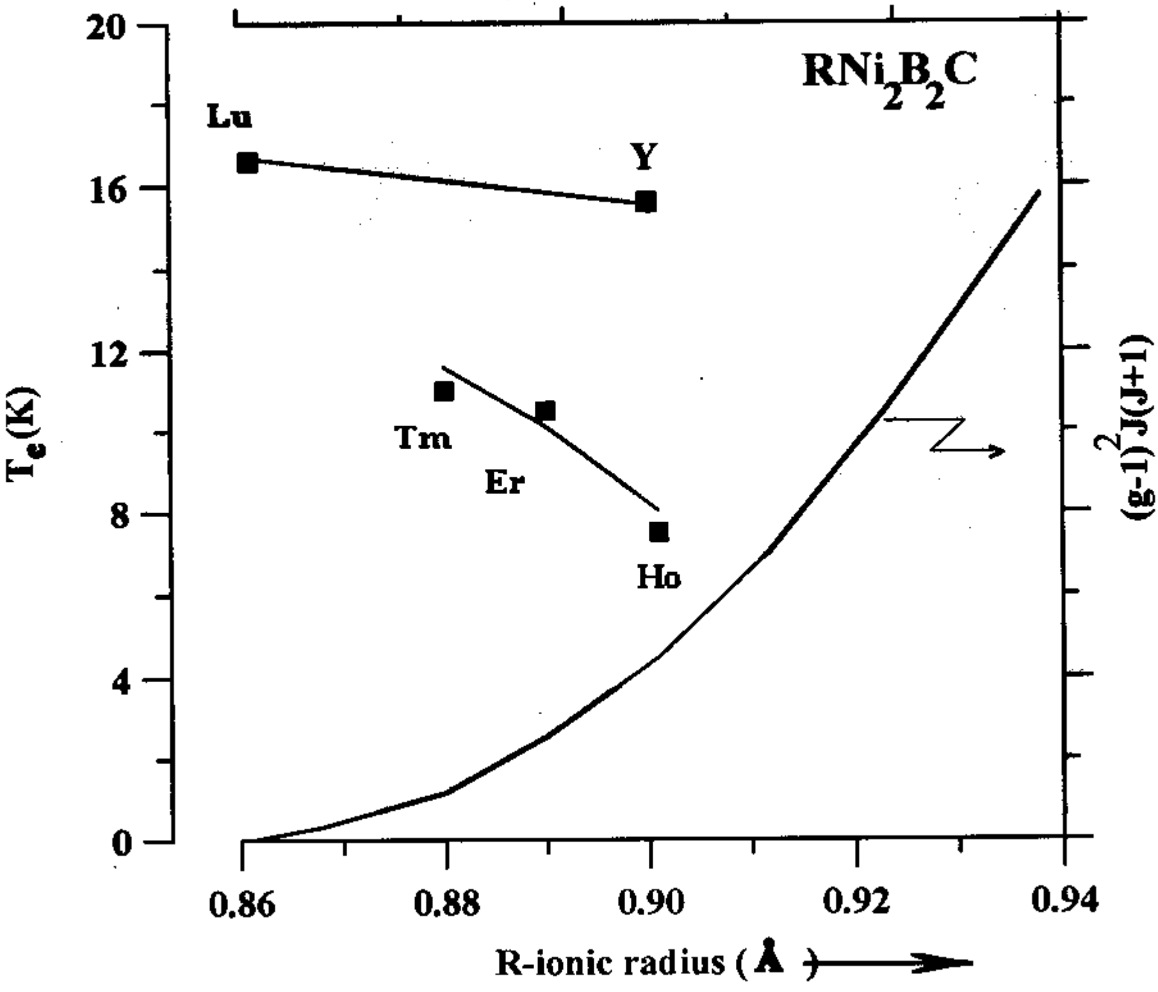
RNi$_2$B$_2$C
Lu
Y
Tm
Er
Ho
20
16
12
8
4
0
T$_c$(K)
(g-1)^{2}J(J+1)
0.86
0.88
0.90
0.92
0.94
R-ionic radius (Å)

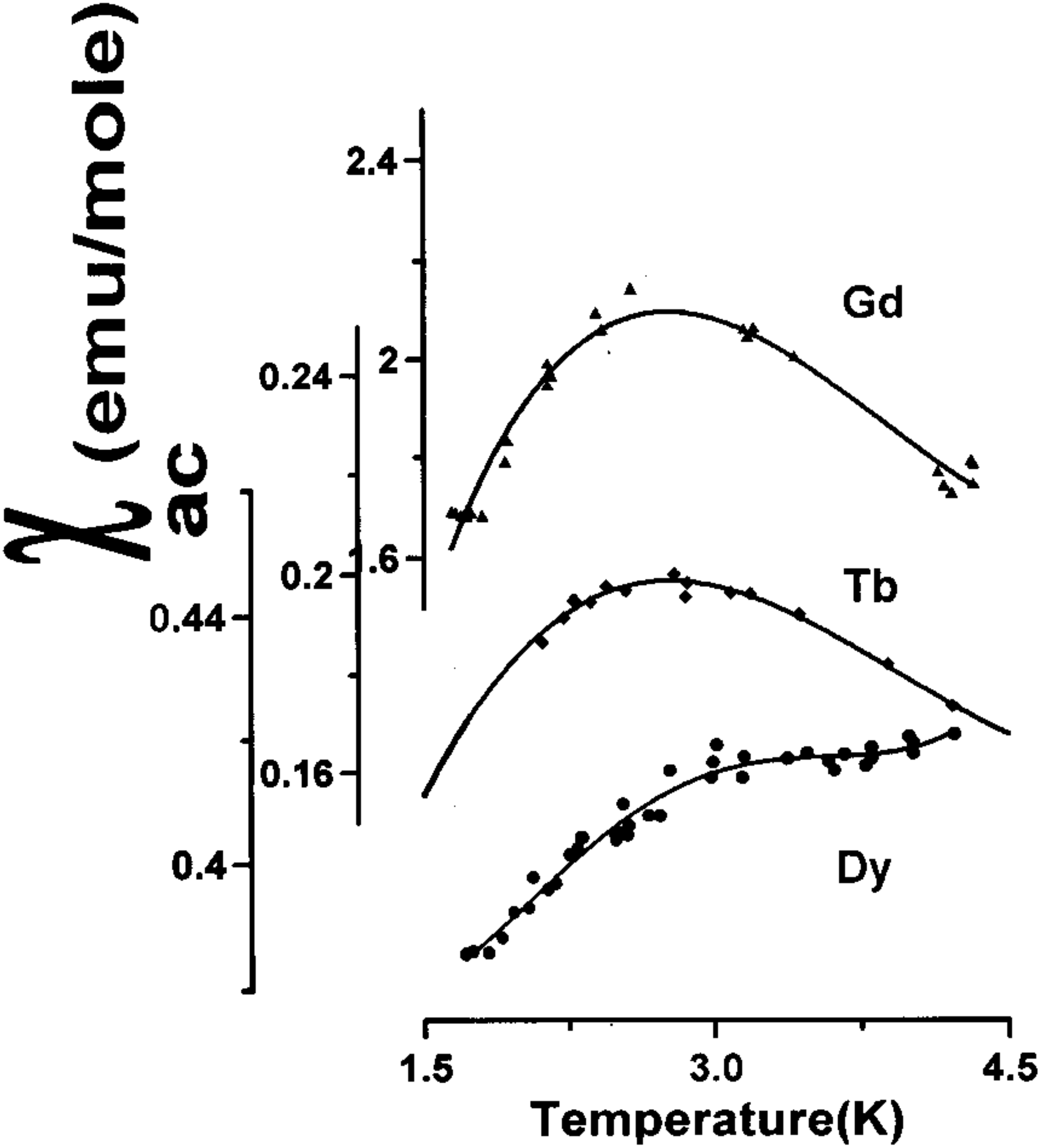
χ_{ac} (emu/mole)
2.4
2
1.6
0.24
0.2
0.16
0.44
0.4
Gd
Tb
Dy
1.5
3.0
4.5
Temperature(K)

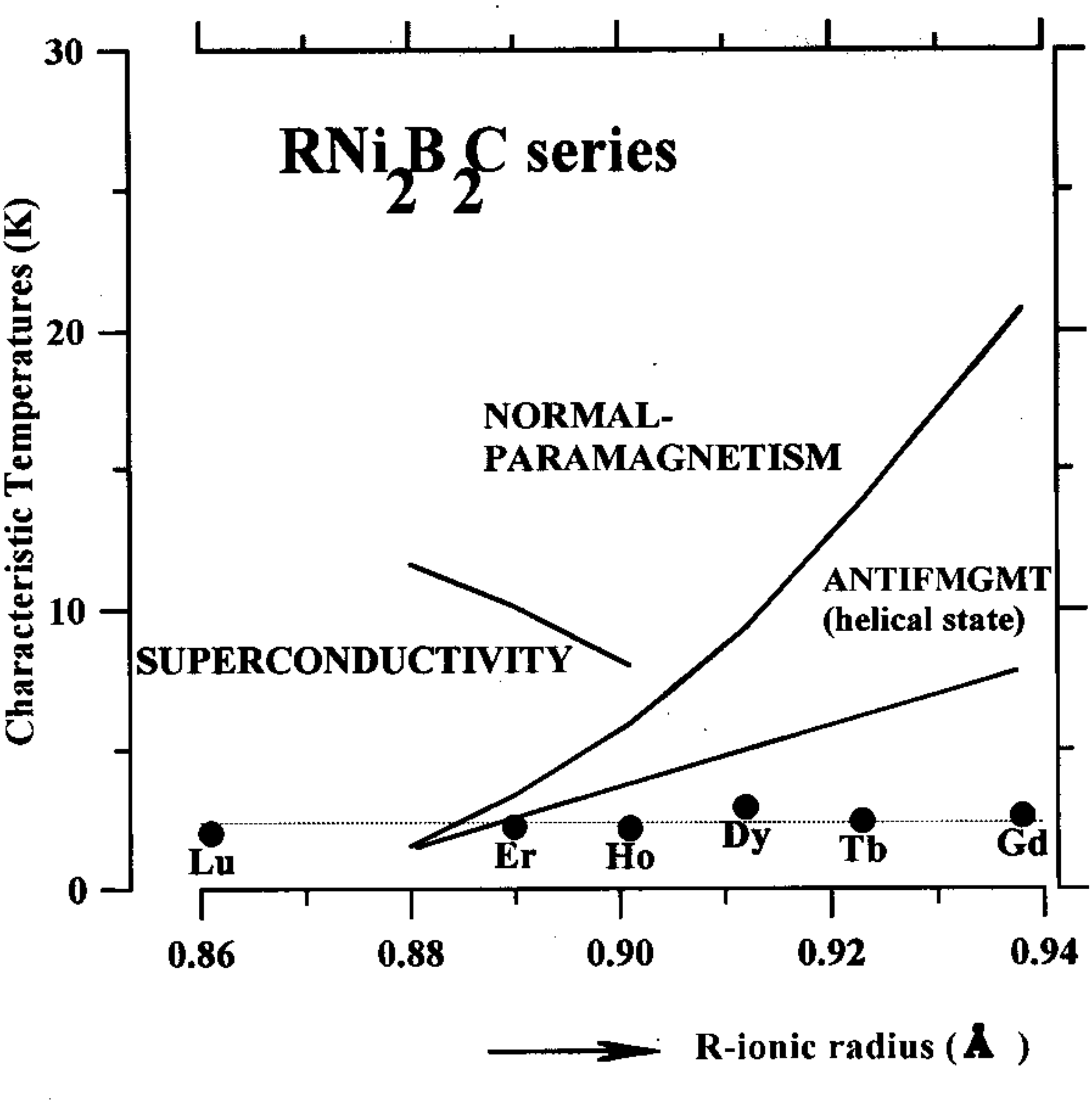
RNi2B2C series
Characteristic Temperatures (K)
30
20
10
0
NORMAL-
PARAMAGNETISM
ANTIFMGMT
(helical state)
SUPERCONDUCTIVITY
Lu
Er
Ho
Dy
Tb
Gd
0.86
0.88
0.90
0.92
0.94
R-ionic radius (Å)